Phosphine-free synthesis of high-quality reverse type-I ZnSe/CdSe core with CdS/Cd_xZn_{1-x}S/ZnS multishell nanocrystals and their application for detection of human hepatitis B surface antigen

2011 Nanotechnology 22 375602

(http://iopscience.iop.org/0957-4484/22/37/375602)

Nanotechnology **22** (2011) 375602 (10pp) doi:10.1088/0957-4484/22/37/375602

Phosphine-free synthesis of high-quality reverse type-I ZnSe/CdSe core with $CdS/Cd_xZn_{1-x}S/ZnS$ multishell nanocrystals and their application for detection of human hepatitis B surface antigen

Huaibin Shen[1,3], Hang Yuan[2,3], Jin Zhong Niu[1], Shasha Xu[1], Changhua Zhou[1], Lan Ma[2] and Lin Song Li[1]

[1] Key Laboratory for Special Functional Materials, Henan University, Kaifeng 475004, People's Republic of China
[2] Life Science Division, Graduate School at Shenzhen, Tsinghua University, Shenzhen 518055, People's Republic of China

E-mail: malan@sz.tsinghua.edu.cn and lsli@henu.edu.cn

Received 22 June 2011
Published 19 August 2011
Online at stacks.iop.org/Nano/22/375602

Abstract

Highly photoluminescent (PL) reverse type-I ZnSe/CdSe nanocrystals (NCs) and $ZnSe/CdSe/CdS/Cd_xZn_{1-x}S/ZnS$ core/multishell NCs were successfully synthesized by a phosphine-free method. By this low-cost, 'green' synthesis route, more than 10 g of high-quality $ZnSe/CdSe/CdS/Cd_xZn_{1-x}S/ZnS$ NCs were synthesized in a large scale synthesis. After the overgrowth of a $CdS/Cd_xZn_{1-x}S/ZnS$ multishell on ZnSe/CdSe cores, the PL quantum yields (QYs) increased from 28% to 75% along with the stability improvement. An amphiphilic oligomer was used as a surface coating agent to conduct a phase transfer experiment, core/multishell NCs were dissolved in water by such surface modification and the QYs were still kept above 70%. The as-prepared water dispersible $ZnSe/CdSe/CdS/Cd_xZn_{1-x}S/ZnS$ core/multishell NCs not only have high fluorescence QYs but also are extremely stable in various physiological conditions. Furthermore, a biosensor system (lateral flow immunoassay system, LFIA) for the detection of human hepatitis B surface antigen (HBsAg) was developed by using this water-soluble core/multishell NCs as a fluorescent label and a nitrocellulose filter membrane for lateral flow. The result showed that such $ZnSe/CdSe/CdS/Cd_xZn_{1-x}S/ZnS$ core/multishell NCs were excellent fluorescent labels to detect HBsAg. The sensitivity of HBsAg detection could reach as high as 0.05 ng ml^{-1}.

S Online supplementary data available from stacks.iop.org/Nano/22/375602/mmedia

(Some figures in this article are in colour only in the electronic version)

1. Introduction

Since the introduction of 'size quantization' by Brus in the 1980s, the synthesis of II–VI colloidal semiconductor nanocrystals (NCs) and their core/shell structures have attracted considerable interest from the scientific community [1–16]. Most of the research is focused on the CdS, CdSe and CdTe NCs and their corresponding core/shell NCs, such as CdSe/CdS [13], CdSe/ZnSe [17], CdSe/ZnS [18, 19],

[3] These authors contributed equally to this paper.

CdSe/CdS/ZnS [18–20] and CdTe/ZnS [21], which are called type-I core/shell NCs, with electrons and holes both located in the narrow bandgap cores. Type-II heterostructured NCs such as CdS/ZnSe [22], ZnSe/CdS [23], CdTe/CdS [24], CdTe/CdSe [25, 26] and CuS/CdS [27] are also investigated due to their unique properties, in which electrons and holes are spatially separated in different components of the heterostructure [22–27]. However, there are only a few examples of the reverse type-I structures, such as CdS/HgS [28], CdS/CdSe [29] and ZnSe/CdSe [30], in which a shell material with a narrower bandgap was deposited onto the core with a wider bandgap. The wavefunction of the electron can dislocate in the shell completely; as a result a significant redshift of the PL can be observed. This property predetermines that reverse type-I nanostructures can be good emitters for their wide range luminescence [30].

There are two important guidelines for nanocrystals: PL quantum yields (QYs) and stability. To improve the PL QYs, different shell materials have been employed to suppress the exciton leakage by forming various core/shell structures. But the stability was still low though the QY was high when thin shells were overcoated [18]. To improve the PL stability, a thick shell is needed indeed. But after growing thicker shells, the QY declined gradually due to the accumulation of structural defects [31]. To form an 'ideal' core/shell with high QY and high stability, core/shell nanocrystals must be formed without structural defects. Consecutive changes of lattice parameters from core to shells can effectively decrease the defects. As a result, they can have not only high QYs and but also high stability.

Herein we report the synthesis of reverse type-I ZnSe/CdSe core/shell NCs and using this structure as the core to synthesize multishell NCs. After the overgrowth of a CdS/Cd_xZn_{1-x}S/ZnS multishell on ZnSe/CdSe NCs, i.e. the wider bandgap materials with a consecutive change of lattice parameters (scheme 1), both electrons and holes transferred from ZnSe to CdSe, Therefore, the QYs were increased from 28% to 75% and the stability was also improved. More than 10 g of high-quality ZnSe/CdSe/CdS/Cd_xZn_{1-x}S/ZnS NCs were synthesized successfully in a large scale reaction using this low-cost, 'green' phosphine-free synthesis route. Even after a phase transfer experiment by using amphiphilic oligomers (polymaleic acid aliphatic alcohol ester) as a surface coating agent, the QYs of ZnSe/CdSe/CdS/Cd_xZn_{1-x}S/ZnS NCs were still kept above 70%. Such water-soluble NCs have high stability in aqueous solution under a wide range of pH, different salt concentrations and thermal treatment at 100 °C. Furthermore, a biosensor system (lateral flow immunoassay system, LFIA) for the detection of human hepatitis B surface antigen (HBsAg) was developed by using this water-soluble NC as a fluorescent label and a nitrocellulose filter membrane for lateral flow.

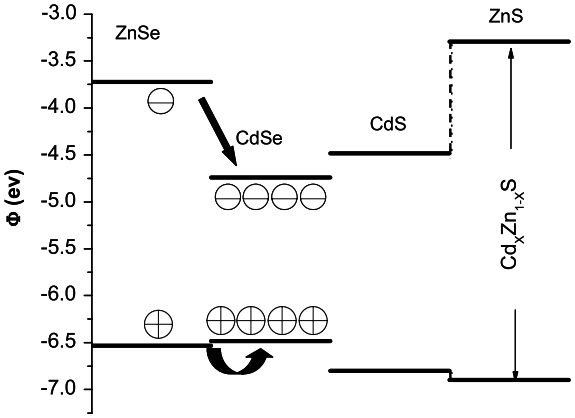

Scheme 1. Energetic band positions of semiconductor material combinations used in this work.

2. Experimental details

2.1. Chemicals

Cadmium oxide (CdO, 99.99%, powder), sulfur (S, 99.98%, powder), 1-octadecene (ODE, 90%), oleic acid (OA, 90%), selenium (Se, 99.99%, powder), zinc oxide (ZnO, 99.99% powder), sodium phosphate dibasic (Na_2HPO_4), sodium phosphate monobasic monohydrate ($NaH_2PO_4H_2O$) and octadecylamine (ODA) were purchased from Aldrich. Sodium chloride (NaCl), hydrochloric acid (HCl), boric acid (H_3BO_3), sodium borate ($Na_2B_4O_710H_2O$) and sodium hydroxide (NaOH) were all analytical grade and obtained from Sagon Biotech Co., Ltd. Tween-20, 2-(*N*-morpholino) ethanesulfonic acid (MES) and bovine serum albumin (BSA) were purchased from Sigma-Aldrich. 1-ethyl-3-(3-dimethylaminopropyl) carbodiimide (EDC) and *N*-hydroxysuccinimide (NHS) were purchased from Pierce. Human hepatitis B surface antigen (HBsAg) and a pair of mouse monoclonal antibodies with different specific sites against HBsAg (HBsAg antibody1 and 2) were purchased from Arista Biologicals Inc. Nitrocellulose membrane, the conjugate pad and absorbent pad were purchased from Millipore. Water with a resistivity of 18 MΩ cm (Purelab Plus, PALL) was used in all the experiments. Polymaleic anhydride, *n*-dodecanol, paraffin oil, hexanes and methanol were obtained from Beijing Chemical Reagent Ltd, China. All reagents were used as received without further experimental purification.

2.2. Preparation of precursors

The Zn, Cd, Se and S precursors used in these experiments were prepared as follows: stock solution for 0.2 M Zn precursor I: a mixture (100 ml in total) of ZnO (1.6274 g, 20 mmol), oleic acid (80 mmol, 20 ml) and 80 ml paraffin oil was loaded into a 250 ml three-necked flask and heated to 300 °C under nitrogen to obtain a colorless clear solution. Stock solution for 0.2 M Zn precursor II: a mixture (375 ml in total) of ZnO (6.1 g, 75 mmol), oleic acid (750 mmol, 210 ml) and 165 ml paraffin oil was loaded into a 500 ml three-necked flask and heated to 300 °C under nitrogen to obtain a colorless clear solution. Stock solution for 0.2 M Cd precursor: a mixture (375 ml in total) of CdO (9.6 g, 75 mmol), oleic acid (750 mmol, 210 ml) and 165 ml paraffin oil was loaded into a 500 ml three-necked flask and heated to 240 °C under nitrogen to obtain a colorless clear solution. Solution for Se precursor: it

was made by degassing Se (1.578 g, 20 mmol), 200 ml of ODE in a 500 ml three-necked flask, then it was heated to 220 °C for 180 min under nitrogen. During this procedure, the color of the precursor changed from transparent to orange, red and finally it turned yellow. Solution for S precursor: the sulfur precursor solution (0.2 M) was prepared by heating a mixture of sulfur (1.92 g, 60 mmol) and ODE (300 ml) to 150 °C. All the above stock solutions were prepared under nitrogen flow.

2.3. Synthesis of ZnSe NCs

High-quality monodisperse ZnSe NCs with zinc blende structure were prepared according to the method reported before [32]. Typically, 10 ml of Se precursor and 10 g paraffin oil were heated to 300 °C under nitrogen gas flow in a 100 ml flask. Next, 5 ml of Zn precursor I solution was injected and the temperature was lowered to 310 °C and maintained for 15 min, then the reaction was stopped. By this approach, ZnSe NCs with an average size of 4 nm were synthesized and an emission wavelength was located at 412 nm.

2.4. Synthesis of ZnSe/CdSe core/shell NCs

The growth of CdSe shell was by the 'successive ion layer adsorption and reaction' (SILAR) method reported before [13]. A typical SILAR synthesis was performed as follows: 30 ml crude ZnSe NCs (4 nm in diameter, 2.8×10^{-4} mol), 30 ml ODE and 20 g of ODA were loaded into a 500 ml reaction vessel. This system was kept at 100 °C under nitrogen flow for 30 min to remove the undesired materials of low vapor pressure. Subsequently, the solution was heated up to 230 °C under nitrogen flow where the shell growth was performed. The amounts of the injection solutions for each step were as follows: Se (0.6 ml)–Cd (0.6 ml)–Se (0.8 ml)–Cd (0.8 ml)–Se (1.05 ml)–Cd (1.05 ml). After that, ZnSe with three-layer CdSe core/shell NCs were obtained. We found that an interval of 10 min between each addition was sufficient for the reaction to be completed, because the UV–vis and PL spectra showed no further changes after this period of time.

2.5. Synthesis of ZnSe/3CdSe/1CdS/6Cd_xZn_{1-x}S/2ZnS core/multishell NCs

The growth of CdS/Cd_xZn_{1-x}S/ZnS multishell was also by the SILAR method reported before [13]. A typical SILAR synthesis was performed as follows: 70 ml of ODE and 30 g of ODA were loaded into a 1000 ml reaction vessel. The ZnSe/3CdSe NCs in hexanes (6.2 nm in diameter, 2.54×10^{-4} mol) were added and the system was kept at 100 °C under nitrogen flow for 30 min to remove the hexanes and other undesired materials of low vapor pressure. Subsequently, the solution was heated to 240 °C under nitrogen flow for shell growth. 1.23 ml of S precursor and 1.23 ml of Cd precursor were injected into the flask for the CdS shell layer growth. Then, S, Cd and Zn precursors were added alternately in the order and amount of S (1.55 ml)—Cd_xZn_{1-x} (a mixture of 1.24 ml Cd and 0.31 ml Zn)—S (1.8 ml)—Cd_xZn_{1-x} (a mixture of 1.44 ml Cd 0.36 ml Zn) for the growth of two monolayers of $Cd_{0.8}Zn_{0.2}S$. Another two monolayers of $Cd_{0.5}Zn_{0.5}S$ alloy shell growth were conducted by adding S, Cd and Zn precursors in the order and amount of S (2.1 ml)—Cd_xZn_{1-x} (a mixture of 1.05 ml Cd and 1.05 ml Zn)—S (2.4 ml)—Cd_xZn_{1-x} (a mixture of 1.2 ml Cd and 1.2 ml Zn). Two monolayers of $Cd_{0.2}Zn_{0.8}S$ alloy shell growth was conducted by adding S, Cd and Zn precursors in the order and amount of S (2.6 ml)—Cd_xZn_{1-x} (a mixture of 0.5 ml Cd and 2.1 ml Zn)—S (3.2 ml)—Cd_xZn_{1-x} (a mixture of 0.6 ml Cd and 2.6 ml Zn). After the temperature was increased to 260 °C, S and Zn precursors were added alternately in the order and amount of S (4.4 ml)–Zn (2.2 ml) to grow the ZnS shell. After that, ZnSe with 12-layer CdSe/CdS/Cd_xZn_{1-x}S/ZnS core/shell NCs were obtained. After refluxing at 260 °C for about one hour, the reaction mixture was allowed to cool down to room temperature. It was precipitated by acetone and followed hexane extraction; the further purification of NCs was by precipitating them with acetone or methanol. The highly pure NCs were obtained by repeating the above purification procedure at least 12 times.

2.6. Preparation of water-soluble NCs

Amphiphilic oligomer polymaleic acid dodecanol ester (PMADE) was synthesized by the reaction of polymaleic anhydride and *n*-dodecanol alcohol [33]. 0.5 g of PMADE was dissolved in 50 ml of distilled water and the pH value of this solution was adjusted to 9 by sodium hydroxide or sodium carbonate. 10 mg of as-synthesized ZnSe/CdSe/CdS/Cd_xZn_{1-x}S/ZnS NCs were purified and dissolved in chloroform and then added to the above polymer solution under vigorous stirring at room temperature. After 24 h, NCs originally dispersed in chloroform were forced to disperse in water during slow evaporation of chloroform, and a clear NC water solution was obtained. Excess polymer molecules were removed by centrifugation at a speed of 17 000 rpm for about 30 min.

2.7. Conjugation of antibodies onto water-soluble nanocrystals

The as-prepared water-soluble ZnSe/CdSe/CdS/Cd_xZn_{1-x}S/ZnS NCs were conjugated with mouse anti-human hepatitis B surface antigen (HBsAg) monoclonal antibody by an EDC/NHS-mediated course [34]. 5.8 mg of water-soluble NCs were mixed with 2 mM NHS and 5 mM EDC in MES buffered saline at pH 4.7 to form an amine reactive sulfo-NHS ester at 37 °C for 30 min. After washing by 50 mM borate buffer (pH = 8.5) under centrifugation (Beckman Avanti 30, Rotor F1202, 16 000*g*, 30 min), the activated water-soluble NCs were dispersed by the same buffer. Then 1.9 mg of HBsAg antibody1 was added. The solution was incubated for 3 h at 37 °C to result in stable amide bonds between the antibody and the water-soluble NCs. Then the conjugates were blocked by adding 5% BSA solution and incubating at 37 °C for 30 min. The obtained conjugate solution was stored at 4 °C before use.

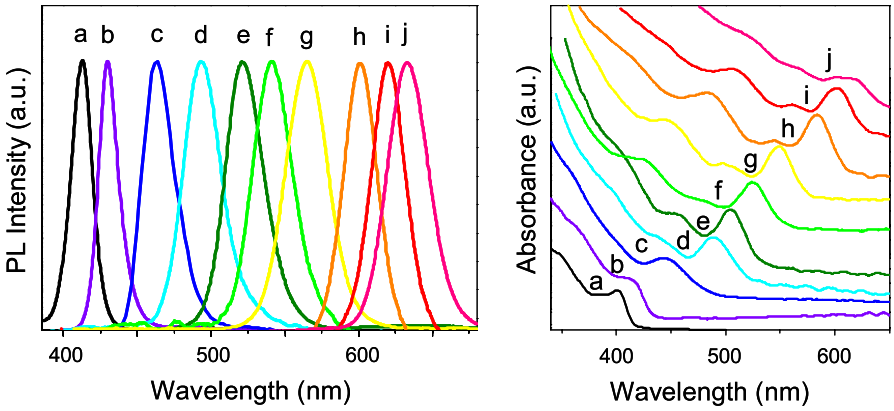

Figure 1. Normalized PL (left, all samples were excited at 365 nm with a UV source) and corresponding absorption (right) spectra of plain ZnSe core NCs (a) and ZnSe/CdSe core/shell NCs with different numbers of monolayers of CdSe shell: (b) 0.1; (c) 0.3; (d) 0.5; (e) 1; (f) 2; (g) 3; (h) 4; (i) 5 and (j) 6.

2.8. Preparation of NCs-lateral flow immunoassay (LFIA) system

To prepare NCs-LFIA strips, HBsAg antibody2 in 10 mM sodium phosphate (pH = 7.4) buffer at 1 mg ml^{-1} was dispensed onto a nitrocellulose membrane as a test line, while the NCs-HBsAg antibody1 conjugates at 0.1 μl/strip were dispensed onto a sample pad. The sample pad was treated with 10 mM sodium phosphate (pH = 7.4) buffer, BSA (0.5%, w/v) and Triton-X100 (2%, w/v) and dried before the dispensation. The dispensation was performed by using the XYZ Dispensing System (BioDot Inc, Irvine, CA). The membrane and sample pad were then dried overnight at room temperature under 10% relative humidity condition. Then the membrane and sample pad were assembled and cut into strips with a width of 3 mm/strip by using the CM4000 Guillotine Cutter (BioDot Inc, Irvine, CA).

2.9. Detection of HBsAg by NC-LFIA strips

To perform the detection, 100 μl of the HBsAg standard solution was added to the end of the sample pad. The NC fluorescence signal on the test line was observed by the fluorescence detector, which has a370 nm LED lamp (1 W) light source, at 20 min after addition. The NC-LFIA assays were performed at various concentrations of HBsAg: 0, 0.05, 0.5, 5 ng ml^{-1}.

2.10. Characterization

UV–vis absorption spectra and PL spectra were recorded using an Ocean Optics spectrophotometer (mode PC2000-ISA). PL spectra were taken using an excitation wavelength of 365 nm. PL quantum yields (QYs) of NCs were measured relative to LD 423 (QY = 68% in ethanol), coumarin 540 (QY = 78% in ethanol) and rhodamine 590 (QY = 95% in methanol), respectively. All the QY data of NCs and dyes were collected through SPEX F212. The NC PL QYs were calculated using the formula as $QY_{NC} = QY_{dye}(I_{NC}/I_{dye})(n_{NC})^2/(n_{dye})^2(1\text{-}10^{-OD_{dye}}/1\text{-}10^{-ODNC})$, where I is the spectrally integrated emission intensity, n is the refractive index and OD is the optical density of the NC or the dye samples (indicated by a subscript). The optical density of the NC samples at the excitation wavelength was within the 0.02–0.05 range. X-ray diffraction (XRD) studies of NCs were carried out with a Philips X′ Pert Pro x-ray diffractometer using Cu Kα radiation ($\lambda = 1.5406$ Å). Transmission electron microscopy (TEM) studies were performed using a JEOL JEM-100CX II microscope with an accelerating voltage of 100 kV. High resolution transmission electron microscopy (HRTEM) observations were performed with a JEOL JEM-2010 microscope with an accelerating voltage of 200 kV. TEM samples were prepared by placing a drop of the NC solution onto a 400 mesh carbon-covered copper grid.

3. Results and discussion

3.1. Synthesis and optical properties of reverse type-I ZnSe/CdSe NCs

For the synthesis of reverse type-I ZnSe/CdSe NCs by this phosphine-free method, selenium needs to be dissolved in 1-octadecene (ODE) and formed an active complex as the precursor before the generation of NCs [32]. Figure 1 shows the evolution of the PL and absorption spectra of the aliquots taken from the reaction solution during the growth of the CdSe shell on the same batch of ZnSe cores with an average diameter of 4 nm. With the increase of the CdSe shell thickness around the ZnSe cores, both the absorption spectra and PL spectra have a systematic redshift. When the increase of the shell thickness is 0.1, 0.2, 0.5, 1, 2, 3, 4, 5 and 6 monolayers, the corresponding PL peaks shift from the original 412 nm, corresponding to the ZnSe cores, to 429, 464, 493, 521, 541, 565, 600, 619 and 632 nm, respectively. The PL emissions from these core/shell NCs span the whole visible range from the violet to the red. Due to the larger conduction band offset in the ZnSe/CdSe system, the charge carriers are mostly delocalized into the CdSe shell with narrower bandgap, especially if thicker shells are formed. The QYs of the core/shell NCs increased steadily from about 45% for

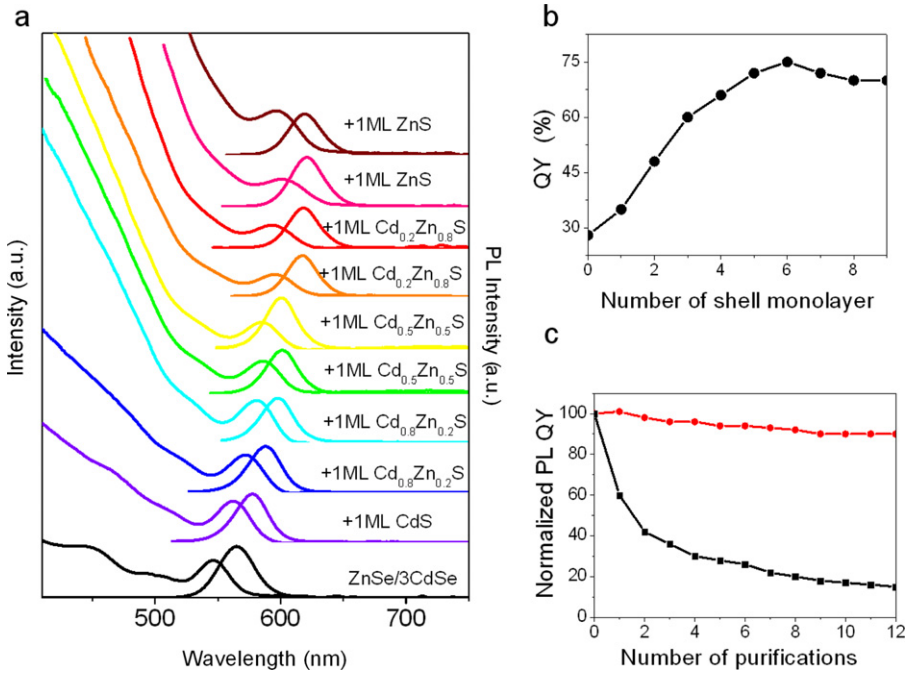

Figure 2. (a) Evolution of the absorption and PL spectra upon consecutive growth of ZnSe/CdSe/CdS/$Cd_xZn_{1-x}S$/ZnS core/shell NCs. (b) Evolution of the PL QY for (a). (c) Evolution of the relative PL QY upon repeated precipitation and redispersion of ZnSe/3CdSe (black squares) and ZnSe/3CdSe/$Cd_xZn_{1-x}S$/ZnS (red dots) core/shell NCs in chloroform solution.

the original core particles to the highest value of about 80% after three full monolayers were formed (figure S1 available at stacks.iop.org/Nano/22/375602/mmedia). If a shell with more than 3 ML is formed, the QY decreases gradually (figure S1 available at stacks.iop.org/Nano/22/375602/mmedia). The lower QYs of the thicker shelled ZnSe/CdSe NCs may originate from lattice imperfections within the shell.

3.2. Synthesis and optical properties of ZnSe/CdSe/CdS/$Cd_xZn_{1-x}S$/ZnS core/multishell NCs

High-quality core NCs are needed for the synthesis of high-quality core/shell NCs due to the quantum yields and monodispersity of core/shell NCs depending on the core quality in a sense [18]. So we choose the above ZnSe/3CdSe NCs as cores to make core/multishell NCs. Figure 2(a) shows the UV–vis and PL spectra of the core/multishell NCs from a typical reaction. PL spectra shift to longer wavelengths compared to the original cores. Such an extensive redshift is also known for several multishell NCs[19] and indicates the extension of the wavefunction into the shell region, which increases the effective size of the core and reduces the quantum confinement felt by the semiconductor wavefunction. It reveals that the absorption and PL spectra show a slight blueshift when the outer layers of ZnS are coated onto the CdS/ZnCdS core/shell NCs. A similar phenomenon was observed before when CdSe NCs were covered with a composite CdS/$Cd_{0.5}Zn_{0.5}S$/ZnS shell [18], and this spectral shift was attributed to partial formation of a $Cd_xZn_{1-x}S$ alloy shell. The formation of the $Cd_xZn_{1-x}S$ alloy will increase the band offset of the shell and hence the effective confinement [35]. Figure 2(b) shows the evolution of the PL QYs for the core/shell NCs. While the QY of the ZnSe/CdSe cores was of about 28% (after washing with hexanes and methanol for five times), it increased to about 75% upon coverage of 1CdS/5$Cd_xZn_{1-x}S$ by the SILAR method. Additional growth of ZnS shells leads to a reproducible decrease in the QY, which is in agreement with former reports [18, 11]. Large scale syntheses of ZnSe/CdSe/CdS/$Cd_xZn_{1-x}S$/ZnS core/shell NCs were conducted in our experiment (figure S2 available at stacks.iop.org/Nano/22/375602/mmedia), and more than 10 g of high-quality core/shell NCs were successfully prepared in one reaction.

It is well known that optical properties of NCs are extremely sensitive to their surface chemistry and chemical environment. The coordinating organic ligands used to passivate the NC's surface during the growth are one of the strong contributors to its optical properties such as QY in emission. For the better performance of NCs in the application of biolabeling and light-emitting devices, purification or ligand exchange is needed to remove excess surface ligands, which may destroy the NC surface and result in the QY decrease [31]. Therefore, multi times washing and precipitation of as-synthesized ZnSe/CdSe/CdS/$Cd_xZn_{1-x}S$/ZnS core/multishell NCs is an important step to test its emission stability. Figure 2(c) clearly shows that the QYs of the multishell nanocrystals do not show any drop upon many times of precipitation from growth solution and redissolution in hexanes. Even though it was almost not dissolvable in hexanes after 12 times precipitation, the QYs still kept almost no change. As a comparison, the QY of ZnSe/3CdSe dropped to 15% of the initial value after 12 times precipitation.

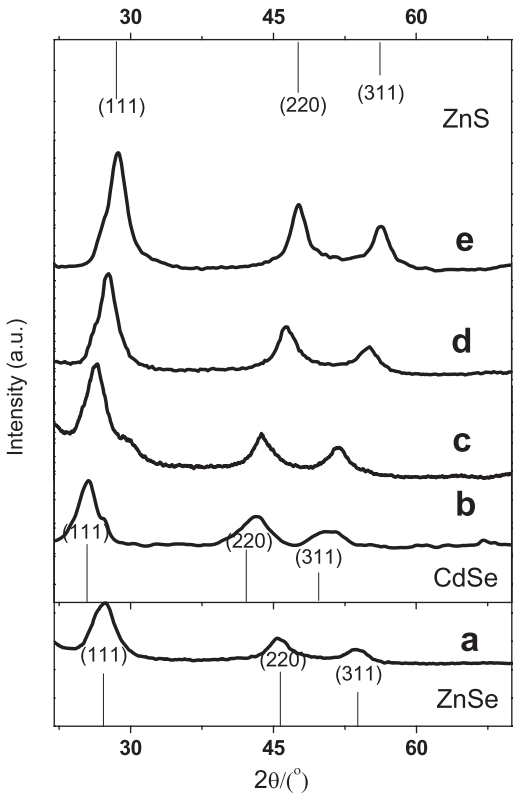

Figure 3. Powder XRD patterns of the different samples: (a) ZnSe NCs which led to the PL spectra in figure 1(a); (b) ZnSe plus three monolayers of CdSe NCs which led to the first absorption and PL spectra in figure 2; (c) ZnSe/3CdSe/CdS NCs which led to the second absorption and PL spectra in figure 2; (d) ZnSe/3CdSe/CdS/$Cd_xZn_{1-x}S$ NCs which led to the eighth absorption and PL spectra in figure 2 and (e) ZnSe/3CdSe/CdS/$Cd_xZn_{1-x}S$/ZnS NCs which led to the last absorption and PL spectra in figure 2.

3.3. Morphology and structural characterization

The XRD patterns of the ZnSe core, ZnSe/3CdSe core/shell and ZnSe/CdSe/CdS/$Cd_xZn_{1-x}S$/ZnS core/multishell NCs are shown in figure 3. For comparison, the standard powder diffraction patterns of zinc blende ZnSe, CdSe and ZnS bulk crystals were provided. Three broad diffraction peaks were observed to correspond to the (111), (220) and (311) planes of the zinc blende phase ZnSe. The XRD patterns shifted from a zinc blende ZnSe-like one to a zinc blende CdSe-like one upon the increase in the CdSe shell thickness. The peak positions were located in the middle of the pure ZnSe and pure CdSe's positions after the growth of three CdSe monolayers. With the growth of another eight monolayers of the shell, it shifted to ZnS-like diffraction patterns totally. It is also clearly shown that XRD peaks get narrower along with the increase of shell thicknesses, which indicates the increase of the nanocrystal's sizes. An obvious peak shift to standard CdSe position and following standard ZnS position has been observed when CdS, $Cd_xZn_{1-x}S$ and ZnS shells were grown on the ZnSe/CdSe core and all samples still kept zinc blende structures. For better comparison, TEM images for ZnSe core, ZnSe/3CdSe core/shell, ZnSe/CdSe/CdS, ZnSe/CdSe/CdS/$Cd_xZn_{1-x}S$ and ZnSe/CdSe/CdS/$Cd_xZn_{1-x}S$/ZnS core/multishell NCs are shown in figure 4. After the growth of three CdSe monolayers, the size was increased from 4±0.3 nm to 6.2±0.8 nm. With the growth of the CdS/$Cd_xZn_{1-x}S$/ZnS shell, the size increased to 12 ± 0.7 nm. The corresponding size-distribution histograms obtained from the TEM images are shown in figures S3(a)–(e) (available at stacks.iop.org/Nano/22/375602/mmedia). As shown in the HRTEM image of ZnSe core NCs, the (111) planes are separated by $d = 0.32$ nm, which is consistent with that of zinc blende ZnSe. After it was overcoated with three monolayers of CdSe, the (111) planes were separated by $d = 0.35$ nm, which was consistent with that of zinc blende CdSe. With the further increase of shell material, the lattice parameters gradual changed to $d = 0.31$ nm, which was consistent with that of (111) planes of zinc blende ZnS. The gradual change of lattice parameters indicated different shell materials were grown onto the core nanocrystals layer by layer. The HRTEM images of core and core/shell NCs show lattice planes that extend straight across the particles, with no evidence of an interface between the core and shells. This implies that the growth of shells occurs in the regime of coherent epitaxy and good crystallinity. To further identify the formation of ZnSe/CdSe/CdS/$Cd_xZn_{1-x}S$/ZnS core/multishell nanocrystals, relative EDS spectrum analysis was performed with Cd–L, Zn–K, S–K and Se–L lines and the elements C, O and Cu were included in the background. Figure S4 (available at stacks.iop.org/Nano/22/375602/mmedia) shows the EDS spectra of ZnSe-based nanocrystals. The content of Se element gradually decreases when the shells began to add. The content of Zn element gradually decreases until the $Cd_xZn_{1-x}S$ shell began to grow. The content of S element increases when CdS, $Cd_xZn_{1-x}S$ and ZnS begin to overcoat on the ZnSe/CdSe nanocrystals. This reveals that different kinds of shells are well controlled when grown on ZnSe cores step by step.

3.4. Preparation of water-soluble ZnSe/CdSe/CdS/$Cd_xZn_{1-x}S$/ZnS core/shell NCs

Additionally, after the growth of the thick multishell, the optical properties of such core/shell NCs were very stable, the high QYs still being retained even after the ZnSe/CdSe/CdS/$Cd_xZn_{1-x}S$/ZnS core/shell NCs underwent the phase transfer process to dissolve in the water phase (figure 5 inset). After phase transfer, the water solution of large scale synthesized high-quality core/multishell NCs are shown in figures 5(B) and (C). The water-soluble NCs were very stable and the QY was still more than 90% of its primary value even after more than six months. A typical TEM image of the core/shell NCs with 10 monolayer shells after phase transfer is shown in figure S5 (available at stacks.iop.org/Nano/22/375602/mmedia). They remained monodisperse in size and no obvious shape change and aggregation was seen. The structure of oligomer-modified fluorescent NCs was illustrated in figure S5 (available at stacks.iop.org/Nano/22/375602/mmedia) (inset). Generally, phase transfer would decrease the QYs of emitting NCs [18, 31]. In our phase transfer experiment, the maintenance of high QYs of ZnSe/CdSe/CdS/$Cd_xZn_{1-x}S$/ZnS core/multishell NCs

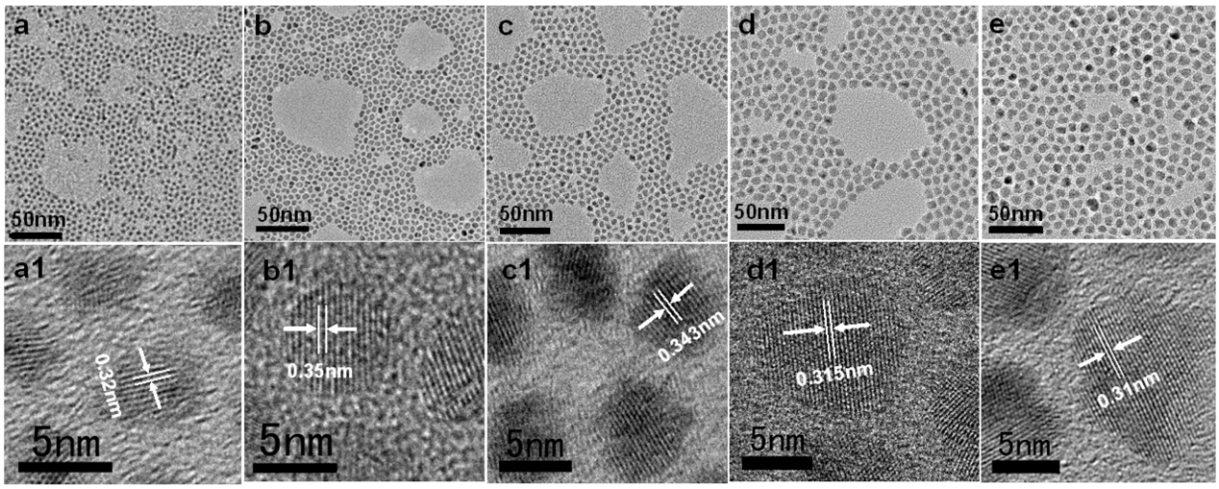

Figure 4. TEM and HRTEM (inset) images of the ZnSe cores and core/shell NCs obtained under typical reaction conditions: (a) TEM images of ZnSe cores; (b): (a) plus three monolayers of CdSe; (c): (b) plus one monolayer of CdS; (d): (c) plus six monolayers of $Cd_xZn_{1-x}S$ and (e): (d) plus two monolayers of ZnS. (a1)–(e1) The corresponding HRTEM of (a)–(e).

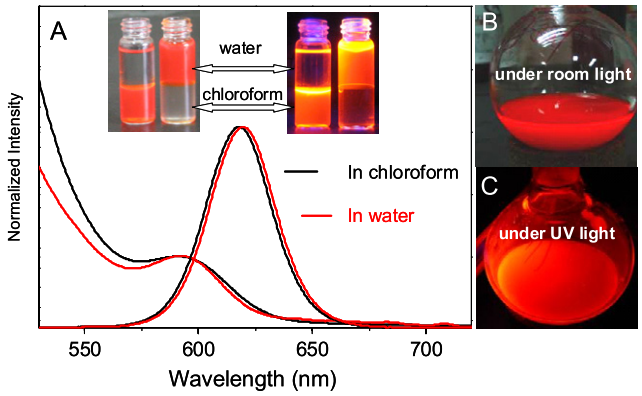

Figure 5. (A) Comparisons of the absorption and PL spectra of ZnSe/3CdSe/CdS/$Cd_xZn_{1-x}S$/ZnS NCs in chloroform (black) and water (red). Inset: a visual comparison of ZnSe/3CdSe/CdS/Cd_xZn_{1-x}S/ZnS NCs in chloroform and water, (B) water solution of large scale synthesized core/multishell NCs under room light and (C) water solution of large scale synthesized core/multishell NCs under UV light (365 nm).

demonstrated both the high stability of NCs and the success of this phase transfer method.

3.5. Characterization of water-soluble ZnSe/CdSe/CdS/$Cd_xZn_{1-x}S$/ZnS core/multishell NCs in physiological conditions

The stability and optical properties of water-soluble ZnSe/CdSe/CdS/$Cd_xZn_{1-x}S$/ZnS core/multishell NCs were tested in physiologically relevant environmental conditions in order to observe whether they were suitable for biological applications. First, temperature-dependent stability was tested because temperature was an important parameter for biological experiments (e.g. polymerase chain reaction (PCR), DNA sensors, cell-incubation studies). As shown in figure 6(A), the fluorescence intensity of the NC water solution slowly decreases when the temperature increases. This result proved that the water-soluble NCs were relatively highly resistant to high temperature. The fluorescence intensity of the NCs' water solution in acidic-to-alkaline pH environments was measured in the following experiment (figure 6(B)). At pH = 4–11 (adjusted by HCl or NaOH), the PMAH-modified water-soluble NCs were stable for months. These water-soluble NCs were also stable in 1 M NaOH (pH = 14) and 0.01 M HCl (pH = 2) solutions for at least 3 h. At pH = 1, the ZnSe/CdSe/CdS/$Cd_xZn_{1-x}S$/ZnS-based water-soluble NCs had lost 30% fluorescence in 1 h. This effect may be attributed to the higher acid etching speed of the water-soluble NCs at low pH. The water solution NCs were also stable in NaCl solutions. In figure 6(C), the fluorescence intensity of these monodisperse NCs is also slowly decreased with the increase of NaCl concentration. Aggregation was not observed for the solution with an NaCl concentration below 0.8 M. It began to aggregate when the NaCl concentration was above 1.0 M. The precipitates of these water solution NCs at high salt concentrations can be re-suspended in solution when the salt concentration is reduced (i.e. by adding distilled water). The colloidal stability of the water-soluble NCs in PBS buffer (pH = 9.0) was estimated as a function of time at 25 °C. As shown in figure 4(d), the fluorescence intensity of the water-soluble NCs only decreased slightly and became constant after approx. 500 h. Furthermore, the FWHM of the water-soluble ZnSe/CdSe/CdS/$Cd_xZn_{1-x}S$/ZnS NCs were almost constant (32 nm) over a long time. This indicated that no deterioration occurred in these water-soluble NCs, and they were stable in PBS solution. All those tests indicated that this water-soluble ZnSe/CdSe/CdS/$Cd_xZn_{1-x}S$/ZnS NCs were suitable for biological applications.

3.6. Demonstration of the water-soluble NCs as fluorescence labels for detecting HBsAg

It is well known that NCs has some advantages over other routine fluorescent labels [5–10]. Being stimulated

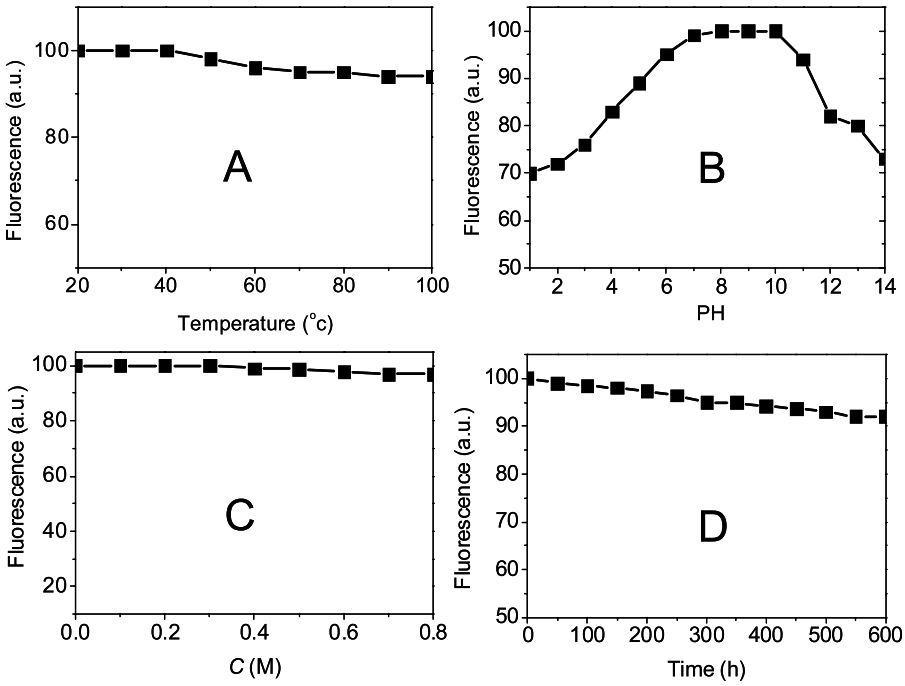

Figure 6. Temperature (A), pH (B), NaCl (C) and PBS buffer (D) stability tests of the water-soluble ZnSe/CdSe/CdS/$Cd_xZn_{1-x}S$/ZnS core/shell NCs.

by a simple light source (even a common LED lamp), it can provide strong visible fluorescence and be easily captured by photographic systems. Therefore, a biosensor system (lateral flow immunoassay system, LFIA, as shown in scheme 2) for the detection of HBsAg was developed by using this water-soluble ZnSe/CdSe/CdS/$Cd_xZn_{1-x}S$/ZnS core/multishell NCs as a fluorescent label and a nitrocellulose filter membrane for lateral flow. The reason why other kinds of NCs were not used successfully in LFIA strips before was lacking the stability and bio-compatibility at the presence of necessary components, such as surfactants, polymers, salts and other blocking reagents. While the ZnSe/CdSe/CdS/$Cd_xZn_{1-x}S$/ZnS core/multishell NCs we made are more reliable for the system, and it has the proper size for running in the matrix of LFIA chromatography. In order to enhance the efficiency of the immunoreaction between antibodies and antigens, shorten the detection time and reduce the detection limit, a microporous polymer membrane was chosen as a matrix for the immunofilter. The membrane provided the following features: a large surface area for antibody immobilization and proper-sized pores in the membrane for forcing the immunoreaction between antibodies and antigens in a space that is small but sufficiently large enough for the flow of the sample solution.

The results shown in figure 7 illustrate the typical images of NCs-LFIA strips from one set of experiments with different concentrations of HBsAg. There is no signal observed in a blank test as shown in figure 7(a), while increased fluorescent signals are observed in (b)–(d). The novel NCs we prepared are demonstrated to be an efficient marker for LFIAs. Moreover, the detection limit for HBsAg in the LFIA system reaches at least 0.05 ng ml^{-1}, which is equal to the

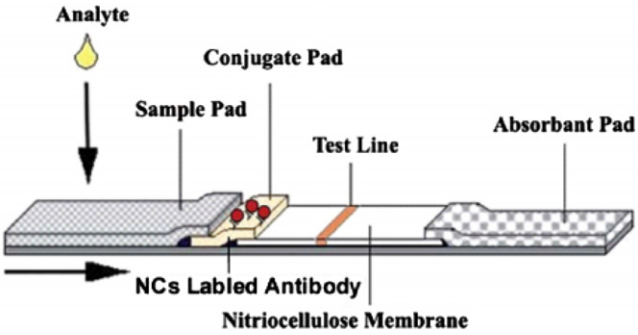

Scheme 2. Schematic representation for the LFIA system.

sensitivity level of ELISA. The increased fluorescent signals at different HBsAg concentrations allow us to study rapid and quantitative analysis for HBsAg in the coming future for clinical purposes. The low detection limit and assay time could have resulted from the high capture efficiency of HBsAg with the microporous membrane and the bright and durable PL of the water-soluble NCs. The achieved water-soluble ZnSe/CdSe/CdS/$Cd_xZn_{1-x}S$/ZnS core/multishell NCs in this study were demonstrated to be a sensitive and reliable novel label material for bioassays.

4. Conclusions

In summary, we have reported the synthesis of highly luminescent, monodisperse reverse type-I ZnSe/CdSe NCs and ZnSe/CdSe core with CdS/$Cd_{1-x}S$/ZnS multishell NCs using phosphine-free precursors. This approach eliminates the need

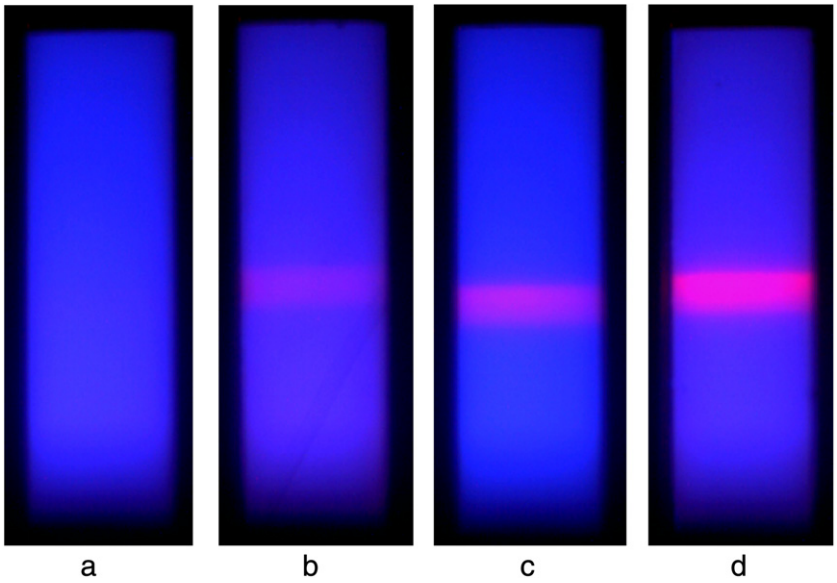

Figure 7. Images of NCs-LIFA strips at different concentrations of HBsAg ((a) blank, (b) 0.05 ng ml^{-1}, (c) 0.5 ng ml^{-1} and (d) 5 ng ml^{-1}) captured by the detection system.

for any air-sensitive, toxic and expensive starting materials such as trioctylphosphine (TOP) and tributylphosphine (TBP). By using this low-cost, 'green' synthesis route, more than 10 g of high-quality ZnSe/CdSe/CdS/$Cd_xZn_{1-x}S$/ZnS NCs were synthesized successfully in a large scale reaction. After the overgrowth of a CdS/$Cd_xZn_{1-x}S$/ZnS multishell on ZnSe/CdSe NCs, the QYs were improved to 75% and the stability was also improved. Even after the phase transfer experiment, the QYs were still kept above 70%. The as-prepared water dispersible core/multishell NCs were highly fluorescent and extremely stable in various physiological conditions. Furthermore, a biosensor system for the detection of HBsAg was developed by using these water-soluble NCs as fluorescent labels and a nitrocellulose filter membrane for lateral flow. The results showed that ZnSe/CdSe/CdS/$Cd_xZn_{1-x}S$/ZnS core/multishell NCs were excellent fluorescent labels to detect HBsAg with a sensitivity of 0.05 ng ml^{-1}.

Acknowledgments

This work was financially supported by the research project of the National Natural Science Foundation of China (21071041), the Program for New Century Excellent Talents in University of Chinese Ministry of Education, the Hi-tech Research and Development Program of China (no. 2006AA03Z359), the Development of New Fluorescent Immunoassay for the Simultaneous Detection to the Residues of Four Varied Veterinary Drugs (SZSITIC grant) and the Development of High Sensitive Fluorescent Immunoassay for the Detection to the Residues of Drugs in the Foods (SZSITIC grant).

References

[1] Peng X, Manna L, Yang W, Wickham J, Scher E, Kadavanich A and Alivisatos A P 2000 *Nature* **404** 59
[2] Murray C B, Norris D J and Bawendi M G 1993 *J. Am. Chem. Soc.* **115** 8706
[3] Mikulec F V, Kuno M, Bennati M, Hall D A, Griffin R G and Bawendi M G 2000 *J. Am. Chem. Soc.* **122** 2532
[4] Talapin D V, Haubold S, Rogach A L, Kornowski A, Haase M and Weller H 2001 *J. Phys. Chem.* B **105** 2260
[5] Yu W W, Chang E, Falkner J C, Zhang J Y, Al-Somali A M, Sayes C M, Johns J, Drezek R and Colvin V L 2007 *J. Am. Chem. Soc.* **129** 2871
[6] Bruchez M, Moronne M, Gin P, Weiss S and Alivisatos A P 1998 *Science* **281** 2013
[7] Chan W C W and Nie S M 1998 *Science* **281** 2016
[8] Zeng R, Zhang T, Liu J, Hu S, Wan Q, Liu X, Peng Z and Zou B 2009 *Nanotechnology* **20** 095102
[9] Jamison J A, Krueger K M, Mayo J T, Yavuz C T, Redden J J and Colvin V L 2009 *Nanotechnology* **20** 355702
[10] Nida D L, Nitin N, Yu W W, Colvin V L and Richards-Kortum R 2008 *Nanotechnology* **19** 035701
[11] Dabbousi B O, Rodriguez-Viejo J, Mikulec F V, Heine J R, Mattoussi H, Ober R, Jensen K F and Bawendi M G 1997 *J. Phys. Chem.* B **101** 9463
[12] Li L S, Pradhan N, Wang Y and Peng X 2004 *Nano Lett.* **4** 2261
[13] Li J J, Wang A Y, Guo W, Keay J C, Mishima T D, Johnson M B and Peng X 2003 *J. Am. Chem. Soc.* **125** 12567
[14] Burda C, Chen X, Narayanan R and El-Sayed M A 2005 *Chem. Rev.* **105** 1025
[15] Deng Z, Yan H and Liu Y 2009 *J. Am. Chem. Soc.* **131** 17744
[16] Deng Z, Mansuripur M and Muscat A J 2009 *Nano Lett.* **9** 2015
[17] Reiss P, Bleuse J and Pron A 2002 *Nano Lett.* **2** 781
[18] Xie R, Kolb U, Li J, Basche T and Mews A 2005 *J. Am. Chem. Soc.* **127** 7480
[19] Shen H, Wang H, Tang Z, Niu J, Lou S, Du Z and Li L S 2009 *Cryst. Eng. Commun.* **11** 1733
[20] Lim S J, Chon B, Joo T and Shin S K 2008 *J. Phys. Chem.* C **112** 1744
[21] Tsay J M, Pfluhoefft M, Bentolila L A and Weiss S 2004 *J. Am. Chem. Soc.* **126** 1926
[22] Ivanov S A, Piryatinski A, Nanda J, Tretiak S, Zavadil K R, Wallace W O, Werder D and Klimov V I 2007 *J. Am. Chem. Soc.* **129** 11708

[23] Alexander N, Maria K, Nishshanka N H and Mikhail Z 2008 *J. Phys. Chem.* C **112** 9301
[24] Schöps O, Thomas N, Woggon U and Artemyev M V 2006 *J. Phys. Chem.* B **110** 2074
[25] Kim S, Fisher B, Eisler H J and Bawendi M 2003 *J. Am. Chem. Soc.* **125** 11466
[26] Seo H J and Kim S-W 2007 *Chem. Mater.* **19** 2715
[27] Li X, Shen H, Li S, Niu J, Wang H and Li L S 2010 *J. Mater. Chem.* **20** 923
[28] Braus M, Burda C and E1-Sayed M A 2001 *J. Phys. Chem.* A **105** 5548
[29] Battaglia D, Li J J, Wang Y and Peng X 2003 *Angew. Chem. Int. Edn* **42** 5035
[30] Zhong X, Xie R, Basche Y, Zhang T and Knoll W 2005 *Chem. Mater.* **17** 4038
[31] Chen Y, Vela J, Htoon H, Casson J L, Werder D J, Bussian D A, Klimov V I and Hollingsworth J A 2008 *J. Am. Chem. Soc.* **130** 5026
[32] Shen H, Wang H, Li X, Niu J, Wang H, Chen X and Li L S 2009 *Dalton Trans.* **47** 10534
[33] Li L S, Zhou C, Shen H, Xu W, Si H, Wang H and Lou S *China Patent Application* No. 200810049551
[34] Fishers 2002 *Bangslab TechNote* 205, Rev. 003
[35] Zhong X, Feng Y, Knoll W and Han M Y 2003 *J. Am. Chem. Soc.* **125** 13559